DOI 10.5162/Ultrasonic2025/B15-a1

Laser Micromachining for Fabrication of Low Frequency Single Crystal Piezocomposites

Tönnis Trittler[1], Christan Endisch[2], Sang-Goo Lee[3], Susan Walter[4], Julian Kober[1], Jochen Hampe[1], Henning Heuer[4], and Moritz Herzog[1]
[1] TUD Dresden University of Technology, Else Kröner Fresenius Center for Digital Health, Dresden, Saxony, Germany
[2] SITEC Industrietechnologie GmbH, Chemnitz, Saxony, Germany
[3] iBULe Photonics Co. Ltd, Incheon, Republic of Korea
[4] Fraunhofer Institute for Ceramic Systems and Technologies, Dresden, Saxony, Germany
toennis.trittler@tu-dresden.de

Abstract: This study investigates laser micromachining of the piezoelectric single crystal material PMN-PT for fabrication of piezocomposites below 20 MHz center frequency. Simulation reveals a drop of thickness coupling coefficient for decreasing wall angles, which are to be expected from such a process. However, absolute pressure output and bandwidth increase due to improved impedance matching resulting from a gradient of acoustic impedance. 2-2 piezocomposite samples were micromachined with depths of $130\ \mu\mathrm{m}$ and further processed to functioning piezocomposites with $8.78\ \mathrm{MHz}$ and $10.58\ \mathrm{MHz}$ center frequency.

Keywords: Laser Micromachining, Ultrashort Laser Pulses, Piezocomposite, Single Crystal, PMN-PT, Ultrasonic Transducer

Motivation

Ultrasonic transducers for medical imaging and Non-destructive Testing (NDT) primarily utilize piezocomposites, which combine active piezoelectric phases with passive polymeric phases [1], [2]. Piezocomposites offer advantages over monolithic material such as increased coupling coefficients, decreased dielectric constant, and lower specific acoustic impedance. Single-crystal piezoelectric materials such as PMN-PT (Lead Magnesium Niobate-Lead Titanate) are appealing due to their properties, but their brittleness complicates micromachining. For applications below 20 MHz, dicing saws are commonly used for fabrication of kerfs in the dice-and-fill process. However, the mechanical processing easily leads to the formation of microcracks, which complicates their handling. In the realm of nonmechanical processing methodologies, laser micromachining utilizing ultrashort laser pulses emerges as a compelling alternative. Laser micromachining of single crystal PMN-PT has been investigated for the fabrication of electro-mechanical actuators [3] as well as high frequency piezocomposites [4], [5] for frequencies above 20 MHz. The goal of our work is to investigate laser micromachining for fabrication of piezocomposites below 20 MHz. Given that this approach entails the introduction of a wall angle to the kerfs, the second objective of this study is to investigate the influence of uneven walls on transducer behavior using finite element (FE) simulation.

Simulation Study: Variation of Wall Angle

A FE simulation study was conducted using COMSOL Multiphysics™ Version 6.3 to investigate the influence of varying wall angles on piezocomposite performance. The frequency domain study covers a range from 1 MHz to 20 MHz. The model is based on a 2-2 piezocomposite unit cell configuration (Fig.1a) with the following geometric parameters: Thickness $t = 130\ \mu m$, pitch $p = 50\ \mu m$, kerf width $k = 30\ \mu m$, and pillar width $b = 20\ \mu m$. The wall angle was systematically varied around the middle axis, maintaining a constant piezoelectric material volume fraction of $40\ \%$ across all configurations. Nine distinct wall angles between 82° and 90° were investigated, with 90° representing the ideal reference case. The total aperture of the modeled structure was 5 mm × 5 mm. Two complementary 2D submodels were implemented for the analysis. The first model comprised a unit cell for electrical impedance calculation under mechanical free conditions on the end faces, using [001] PMN-28PT as piezoelectric material. Material parameters for PMN-PT are based on the results from Joh et al. [6]. Epotek 301-2 was used as passive phase with material constants $\rho = 1158\ \mathrm{kg/m^3}$, $v_\mathrm{l} = 2103\ \mathrm{m/s}$, $v_\mathrm{s} = 1082\ \mathrm{m/s}$. The second model adds a backing (Material: Ellsworth EP1121; $\rho = 1127\ \mathrm{kg/m^3}$, $v_\mathrm{l} = 2826\ \mathrm{m/s}$, $v_\mathrm{s} = 1484\ \mathrm{m/s}$; thickness $450\ \mu m$) and water domain for Transmitting Voltage Response (TVR) determination. This comprehensive model incorporates a circular water domain on top of the trans-

DOI 10.5162/Ultrasonic2025/B15-a1

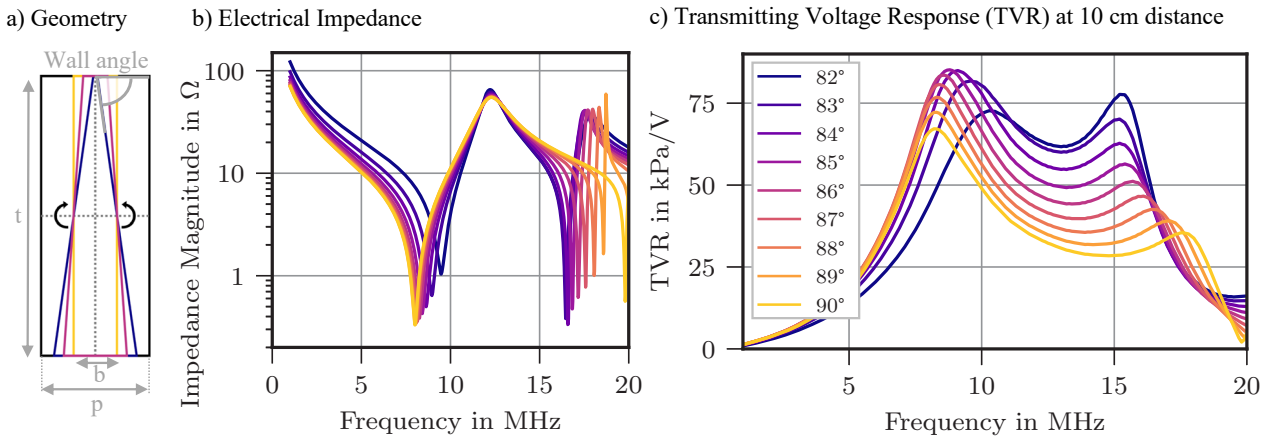

Fig. 1: Simulated unit cell geometry and resulting electrical impedance and transmitting voltage response curves for the simulation study.

ducer with perfectly matched layer and external pressure field calculation at 10 cm distance. The primary transducer characteristics evaluated were the thickness coupling coefficient k_t from electrical impedance data (see (1), according to IEEE standard [7]), center frequency f_c for the main thickness resonance from TVR, and the absolute -3 dB bandwidth from TVR.

$$k_\mathrm{t} = \sqrt{\frac{\pi}{2}\frac{f_\mathrm{r}}{f_\mathrm{a}}\tan\left(\frac{\pi}{2}\frac{f_\mathrm{r}-f_\mathrm{a}}{f_\mathrm{a}}\right)} \qquad (1)$$

The electrical impedance and TVR spectra for different wall angles are presented in Fig.1(b,c), while Fig.2 shows the extracted transducer characteristics.

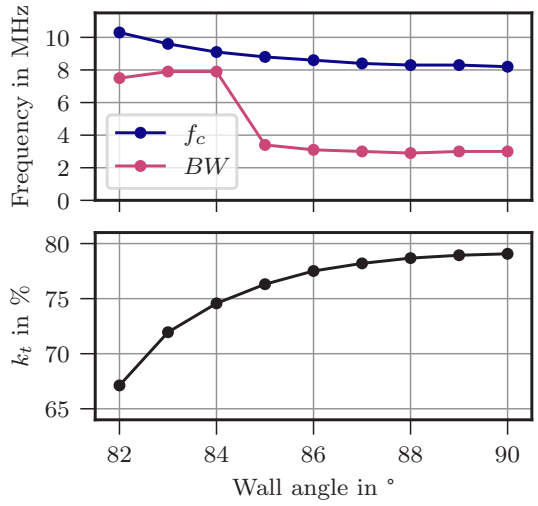

Fig. 2: Center frequency f_c, absolute bandwidth BW (-3 dB) and thickness coupling coefficient k_t.

The electrical impedance analysis reveals that the resonance frequency f_r shifts towards higher frequencies with decreasing wall angles, while the antiresonance frequency f_a remains constant. This behavior results in a decrease of the coupling coefficient k_t. Additionally, the polymer's spurious resonance exhibits a shift from 20 MHz to 17 MHz with decreasing wall angle. The TVR analysis demonstrates that the center frequency f_c shifts from 8.2 MHz to 10.3 MHz, correlating with the f_r shift observed in the electrical impedance data. The maximum TVR value shows an increase from 67.2 kPa/V at 90° to 85.2 kPa/V at 84°, followed by a decrease, though the value at 82° remains above the 90° reference. Concurrent with these changes, the polymer's spurious resonance shifts to lower frequencies with increasing amplitude, eventually exceeding the center resonance at 82°. A significant increase in the -3 dB bandwidth occurs between 84° and 85°. Overall, we observe on the one hand lower k_t with decreasing wall angle, but improved acoustic output in terms of maximum output pressure and bandwidth. This could be attributed to two competing mechanisms affecting transducer performance with decreasing wall angles. The first mechanism manifests as decreased thickness resonance efficiency with lower wall angles due to the changing aspect ratio and therefore increased lateral vibration modes. However, this is counterbalanced by the second mechanism, where improved impedance matching occurs due to lower impedance mismatch at the interface. The data suggests that this gradient of acoustic impedance along the thickness direction benefits transducer performance. The tradeoff between these opposing effects suggests an optimal wall angle range of around 84° for the investigated dimensions, maximizing bandwidth while

DOI 10.5162/Ultrasonic2025/B15-a1

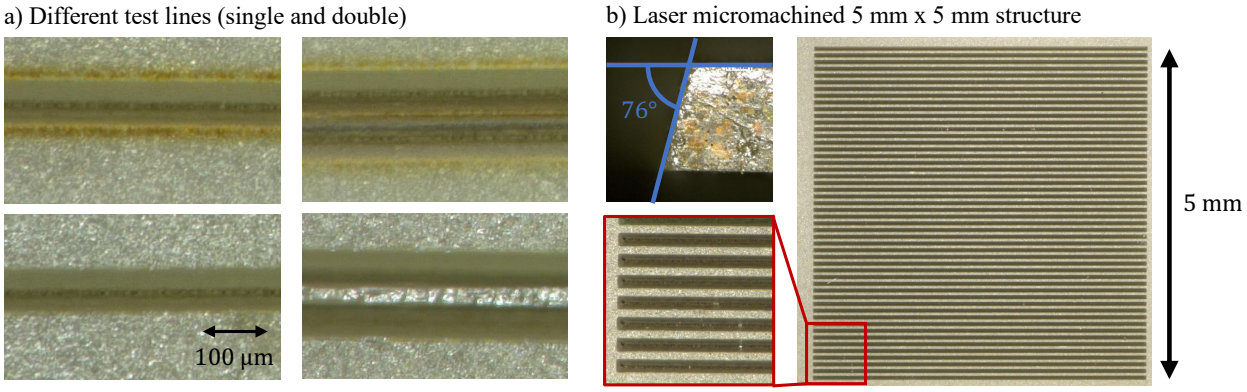

Fig. 3: Microscopy images showing the laser micromachined structures for a) the first ablation tests before and after ultrasonic cleaning and b) the finally produced structures for further piezocomposite fabrication.

maintaining acceptable coupling efficiency.

Laser Micromachining

Micromachining tests were performed using a SITEC Mikrolas machine equipped with a green laser ($\lambda = 514$ nm) operating with femtosecond pulses (Spirit100SHG). The optical setup consisted of a ScanLab intelliSCAN10 optic with 100 mm focal length. The system operated at an average power of 20 W (at 2 MHz) with a spot size of 12 μm.

Preliminary ablation tests were conducted to determine the power threshold and the fluence of the laser pulses for ablation. Based on these results single kerfs were ablated, followed by two parallel kerfs (see Fig. 3). Removal of debris and color changes around the kerfs was tried to remove by ultrasonic cleaning. This lead to breaking off of tips, as can be seen in Fig.3 a (bottom right). Therefore, a cleaning strategy using laser pulses below the ablation threshold was successfully implemented, leading to clean surfaces around the kerfs without breaking of tips. The final process parameters included a laser track spacing of 5 μm, operating frequency of 31.25 kHz, scan speed of 0.156 m/s, and pulse power set to 80%. Due to the heat sensitivity of the PMN-PT, the kerfs were not ablated one after another but layer by layer, quasi-simultaneously to distribute the heating. These parameters enabled the achievement of depths exceeding 120 μm without visible damage to the material.

Based on the test kerf results, a 2-2 piezocomposite structure was fabricated with parallel kerfs in one direction. The structure featured a pitch $p = 100\mu$m, wall angle of $76°$, and approximate depth of 130μm, covering a 5 mm $\times$ 5 mm area in total.

Piezocomposite Fabrication and Characterization

After laser micromachining, the produced samples were further processed into piezocomposites. First, the kerfs were filled with Epotek 301-2. The samples were subsequently lapped to achieve desired thicknesses of 130 μm and 200 μm, followed by chrome-gold metallization through sputtering. Poling was performed at 6 kV/cm, increased from an initial 5 kV/cm due to insufficient poling at lower fields. This could be attributed to non-uniform electrical field distributions due to the wall slope. The resulting structures are shown schematically in Fig. 4a.

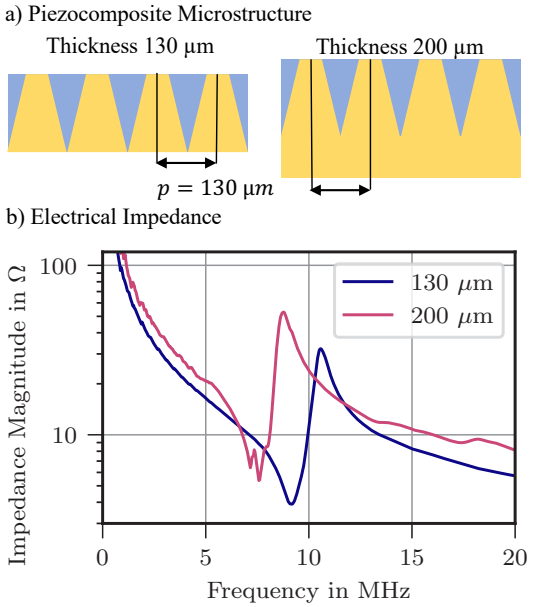

Fig. 4: Geometry (a) and electrical impedance measurement (b) of fabricated piezocomposite samples.

Tab. 1: Derived piezocomposite characteristics.

Thickness	$\varepsilon_{\mathrm{r}}^{\mathrm{T}}$	k_{t}	f_{a}
130 μm	1317	54.0 %	10.58 MHz
200 μm	1927	54.4 %	8.78 MHz

The thinner piezocomposite has kerfs extending to the bottom, whereas for the thicker piezocomposite a bridge of PMN-PT remains. These microstructures correspond to a piezoelectric volume fraction of $67\ \%$ for the thin piezocomposite and $78\ \%$ for the thicker one. Electrical impedance characterization was conducted using an Agilent 4294A impedance analyzer with an Agilent 16334A test fixture. The coupling coefficient k_t was derived according to (1), while the relative permittivity $\varepsilon_{\mathrm{r}}^{\mathrm{T}}$ was calculated from capacitance measurements at $1\ \mathrm{kHz}$. The antiresonance frequency serves as an indication of the center frequency of the piezocomposites. The complete results are summarized in Table 1. For comparison, the monolithic material exhibited a coupling coefficient k_t of $54.2\ \%$ and relative permittivity ϵ_{33} of 4842. The coupling coefficient of the piezocomposites does not exceed the one for pure PMN-PT, but the relative permittivity is significantly smaller.

Conclusion

Our results demonstrate that depths of $130\ \mu\mathrm{m}$ can be achieved with laser micromachining of PMN-PT, making the process suitable for piezocomposites operating at frequencies below 20 MHz. While the piezocomposite manufacturing was successful, the wall angle was limited to $76°$, corresponding to an aspect ratio of approximately 2, which did not yield coupling coefficient advantages over the monolithic material. This is in alignment with the observed drop in coupling coefficients with decreasing wall angle in the simulation results. Nevertheless, other advantages of piezocomposites persist, including lower dielectric constant and reduced specific acoustic impedance. Future improvements to this work will focus on enhancing the wall angle through optimization of the laser process parameters. Additional developments will include extension to 1-3 piezocomposite structures and exploration of different materials, such as [011]-poled material, which is better suited for 2-2 piezocomposites [8]. Furthermore, the fabrication of transducers from the existing samples will enable evaluation of acoustic output characteristics.

Acknowledgment

This research was supported by the European Union and tax revenues on the basis of the budget adopted by the Saxon State Parliament as part of the project HYBRIDECHO under the grant number 100689694. This research was also supported by the Material Technology Development Program (No. 2410004461) through the Korea Evaluation Institute of Industrial Technology (KEIT).

References

[1] P. Kabakov, T. Kim, Z. Cheng, X. Jiang and S. Zhang, 'The versatility of piezoelectric composites,' *Annual Review of Materials Research*, vol. 53, no. 1, pp. 165–193, 3rd Jul. 2023. DOI: 10.1146/annurev-matsci-080921-092839.

[2] T. Herzog, S. Walter, S.-G. Lee, J.-H. Lee, F. Schubert and H. Heuer, 'High-performance ultrasonic transducers based on PMN-PT single crystals fabricated in 1-3 piezo-composite technology,' presented at the 2019 International Congress on Ultrasonics, Bruges, Belgium, 2019, p. 032 007. DOI: 10.1121/2.0001159.

[3] G. Piredda, S. Stroj, D. Ziss *et al.*, 'Micromachining of PMN-PT crystals with ultrashort laser pulses,' *Applied Physics A: Materials Science and Processing*, vol. 125, no. 3, Mar. 2019, Publisher: Springer Verlag, ISSN: 14320630. DOI: 10.1007/s00339-019-2460-9.

[4] Z. Lei, G. Xu, J. Liu, Y. Liu and X. Ji, 'Micromachining of high-quality PMN–PT/epoxy 1–3 composite for high-frequency (30 MHz) ultrasonic transducer applications,' *IEEE Transactions on Ultrasonics, Ferroelectrics, and Frequency Control*, vol. 70, no. 11, pp. 1563–1573, Nov. 2023. DOI: 10.1109/TUFFC.2023.3320652.

[5] Z. Lei, G. Xu, J. Liu and X. Ji, 'Low-stress ultrafast laser micromachining for high-frequency PMN–PT/epoxy composite transducers,' *IEEE Sensors Journal*, vol. 24, no. 5, pp. 5873–5884, 1st Mar. 2024. DOI: 10.1109/JSEN.2023.3347881.

[6] C. Joh, J. Kim and Y. Roh, 'Determination of the complex material constants of PMN–28%PT piezoelectric single crystals,' *Smart Materials and Structures*, vol. 22, no. 12, p. 125 027, 1st Dec. 2013. DOI: 10.1088/0964-1726/22/12/125027.

[7] 'Ieee standard on piezoelectricity,' *ANSI/IEEE Std 176-1987*, 1988. DOI: 10.1109/IEEESTD.1988.79638.

[8] Y. Je, M. Sim, Y. Cho, S.-G. Lee and H.-S. Seo, 'Theoretical and experimental studies on sensitivity and bandwidth of thickness-mode driving hydrophone utilizing a 2-2 piezoelectric single crystal composite,' *Sensors*, vol. 23, no. 7, p. 3445, 24th Mar. 2023. DOI: 10.3390/s23073445.